

## Superabundant vacancy formation in Nb–H alloys; resistometric studies

This article has been downloaded from IOPscience. Please scroll down to see the full text article.

2004 J. Phys.: Condens. Matter 16 1335

(<http://iopscience.iop.org/0953-8984/16/8/017>)

View [the table of contents for this issue](#), or go to the [journal homepage](#) for more

Download details:

IP Address: 129.252.86.83

The article was downloaded on 27/05/2010 at 12:46

Please note that [terms and conditions apply](#).

# Superabundant vacancy formation in Nb–H alloys; resistometric studies

Hideyuki Koike, Yoshiyuki Shizuku, Akio Yazaki and Yuh Fukai<sup>1</sup>

Department of Physics, Chuo University, Kasuga, Bunkyo-ku, Tokyo 112-8551, Japan

E-mail: fukai@phys.chuo-u.ac.jp

Received 3 November 2003

Published 13 February 2004

Online at [stacks.iop.org/JPhysCM/16/1335](http://stacks.iop.org/JPhysCM/16/1335) (DOI: 10.1088/0953-8984/16/8/017)

## Abstract

The formation of superabundant vacancies (SAVs; vacancy–hydrogen clusters) was studied in Nb–H alloys by means of resistivity measurements as a function of temperature, pressure and H concentration. The formation energy of a vac–H cluster ( $0.3 \pm 0.1$  eV), which is 1/10 of the formation energy of a vacancy in Nb, is explained tentatively as being the consequence of six H atoms trapped by a vacancy with the average binding energy of 0.46 eV/H atom. The SAVs were introduced from the external surface, and transported into the interior by direct bulk diffusion and/or by fast diffusion along dislocations. The activation volumes for the formation and migration of vac–H clusters were determined to be 3.7 and 5.3 Å<sup>3</sup>, respectively.

## 1. Introduction

Vacancies in metals play a key role in the diffusion of metal atoms; the diffusivity is given by the product of the concentration and diffusivity of vacancies. Both the formation and migration of vacancies are thermal activation processes, and the equilibrium concentrations of vacancies are generally low, being  $\sim 10^{-4}$  even at the melting point. In 1993, we discovered that, in the presence of interstitial hydrogen atoms, the concentration of vacancies in Ni and Pd became extremely high, as high as  $\sim 10$  at.% [1]. This phenomenon has since been observed in a large number of M–H alloys, and is now called superabundant vacancy (SAV) formation [2–18]. A survey of the work performed heretofore was given in our recent review papers [19, 20]. For this stunning increase of the equilibrium vacancy concentration, we inferred that the reduction of the vacancy formation energy caused by H trapping should be responsible [17, 18], based on our background knowledge of vacancy–hydrogen (vac–H) interactions accumulated in the 1980s in connection with fusion materials research. For a review of H interaction with radiation-induced defects, see, e.g. [21, 22]. Due to attractive interaction with interstitial H atoms, vacancies in M–H alloys should be formed as vac–H clusters, with multiple H atoms trapped

<sup>1</sup> Author to whom any correspondence should be addressed.

by each vacancy in the form  $\text{vacH}_r$ ,  $r \leq 6$ , and their formation energy ( $e_f^{\text{cl}}$ ) should be lower than the vacancy formation energy ( $e_f^{\text{v}}$ ) by the sum of the binding energies ( $\sum_i e_{\text{bi}}$ ). In Ni, for example, if we adopt the reported binding energies,  $e_b = 0.44$  eV for the first two H atoms and 0.28 eV for the additional four H atoms trapped by a vacancy [23], and a vacancy formation energy of 1.56 eV [24], we arrive at a formation energy of a vac–H cluster,  $e_f^{\text{cl}} \approx -0.44$  eV. The reduction of the formation energy is thus appreciable, and easily leads to the enhancement of the equilibrium concentration by many orders of magnitude. The situation is very similar in other metals.

The SAV formation is in fact one of the most basic properties of the M–H system. As structures containing SAVs are generally lower in energy, all M–H alloys should assume these defect structures whenever the kinetics allows, and in consequence come to exhibit such properties as enhanced M-atom diffusion and creep [5, 19, 25]. A gradual degradation of electroplated copper films, a serious problem in present-day technology, is also believed to be of the same origin. Thus, elucidation of the formation and properties of SAVs is of crucial importance both in physics and in materials science of the M–H system.

Up to now, most of our experiments on the SAV formation have been done by measuring the x-ray diffraction (XRD) at high temperatures ( $T \leq 1000$  °C) and high hydrogen pressures ( $p_{\text{H}} \leq 5$  GPa). High temperatures are needed to allow the introduction of vacancies by diffusion, and high hydrogen pressures to confine H atoms in solution at such high temperatures. Gradual lattice contractions amounting to a few per cent were observed over several hours, from which the vacancy concentrations of  $\sim 10$  at.% were deduced.

These experiments have played a crucial role in establishing the generality of this phenomenon, but suffer from some inherent ambiguities. First, lacking knowledge of the rate of lattice contraction per given concentration of vac–H clusters, we have to approximate this by the corresponding quantity reported for pure metals. To what extent this approximation is valid is not very clear, however. Second, under a given  $p_{\text{H}}$ ,  $T$  condition, namely under a given chemical potential of hydrogen, the concentration of interstitial hydrogen may also vary with the formation of vacancies. Both these processes cause lattice parameter changes, and their separate determination from XRD data alone is not possible. Thus, in order to investigate the quantitative aspects of the SAV formation process, some other experimental methods have to be developed.

The purpose of this paper is to report such experiments performed on Nb–H alloys. Fortunately, there are cases, so-called anomalous bcc metals (Fe, V, Nb, Ta), where the migration energy of vacancies is so low ( $\sim 0.5$  eV) [24] that the SAV formation may proceed at reasonably low temperatures. Thus, in  $\alpha$ -Fe, after heat treatments at between 200 and 600 °C and a hydrogen pressure of 1.7 GPa, a total of 0.1–1.5 at.% hydrogen trapped by vacancies was observed by thermal desorption spectroscopy [6]. Vanadium, Nb and Ta provide more interesting possibilities, because in addition to the high mobility of vacancies, hydrides of these metals are very stable. Thus, the introduction of vac–H clusters can be realized at moderate temperatures under ambient conditions. The advantage of working at ambient pressure is that it allows the adoption of a variety of experimental techniques for characterizing the SAV formation. For example, the electrical resistance, which is much more sensitive than the lattice parameter to the vacancy formation, can be conveniently utilized, on carefully fabricated single-crystal specimens of prescribed hydrogen concentrations.

The present work is a first report of SAV formation in Nb–H alloys at reasonably low temperatures without application of high hydrogen pressures. From the temporal variation of the electrical resistivity, the source and the migration process of vacancies have been characterized, and from the magnitude of the resistivity increase the dependence of the equilibrium vacancy concentration on temperature and H concentration has been deduced.

Some high-pressure experiments have also been performed to determine the activation volume for the formation and migration of vac–H clusters.

## 2. Experimental methods

The main body of the experiments were performed using specimens cut out from a Marz grade single crystal of Nb purchased from MRC, and some additional experiments using a polycrystalline wire of 99.99% purity purchased from JMC. The sample size was 0.17 mm × 0.5 mm × 6 mm for most single crystals and diameter 0.5 mm × 50 mm for polycrystals. Hydrogenation was performed by electrolysis at room temperature in a 0.2 N H<sub>2</sub>SO<sub>4</sub> solution. The H concentration attained after variable charging times was determined by a gas-extraction method.

Temporal variation (increase) of the electrical resistance was measured at several temperatures up to 350 °C, over a period of time extending to 250 ks (~70 h). In these measurements, a sample was placed in a specially designed quartz tube and was heated by an infrared lamp furnace stepwise to a prescribed temperature. After a few minutes of the initial heating period, the temperature was controlled to within ±0.2 °C. The tube was filled with the equilibrium pressure of H<sub>2</sub> gas to ensure constant H concentration over the whole period of the measurement. The resistance measurement was made by a combination of a KEITHLEY 2400 Sourcemeter and 2182 Nanovoltmeter, which allowed programmed measurements every 1 s, each unit of measurement consisting of ten repetitions of alternating polarities. The resistance measurement itself was sufficiently stable over indefinite lengths of time; the maximum measuring time and temperature were limited by the oxidation of samples characterized by rapid increase of the resistivities at high temperatures (≥350 °C).

Resistance measurements under high pressures were made to 5 GPa using a cubic-anvil press Oz-F1 in our laboratory. This press compresses a cubic sample cell of 8 mm edge length from six perpendicular directions to produce a nearly homogeneous pressure at the centre. A single-crystal sample of miniature size, measuring e.g. 0.17 mm × 1.5 mm × 0.4 mm, was sandwiched between NaCl plates (H sealants) and a pair of graphite disc heaters, and this assembly was encased in a cell made of a solid pressure-transmitting medium (pyrophyllite). The temperature was controlled to within ±0.5 °C during each run.

## 3. Experimental results

### 3.1. Kinetics of vacancy formation

Figure 1 shows a record of the resistivity change as a function of time for a single-crystal sample of NbH<sub>0.21</sub> measured at 300 °C. The resistance increase occurs in two stages, one having a small time constant ( $\tau_1 \approx 1$  ks) and the other having a large time constant ( $\tau_2 \approx 30$  ks). The presence of these two stages indicates that two different mechanisms of vacancy formation are operating.

Anticipating that the fast process is due to formation from some internal sources such as dislocations and the slow process from the external surface, measurements were made subsequently on samples of several different thicknesses. The observed curve was fitted to the sum of three components,  $\Delta\rho(t) = \Delta\rho_1(t) + \Delta\rho_2(t) + \Delta\rho_{ox}(t)$ , where  $\Delta\rho_1(t)$  is the fast component expressed as

$$\Delta\rho_1(t) \approx \Delta\rho_1(1 - e^{-t/\tau_1}), \quad (1)$$

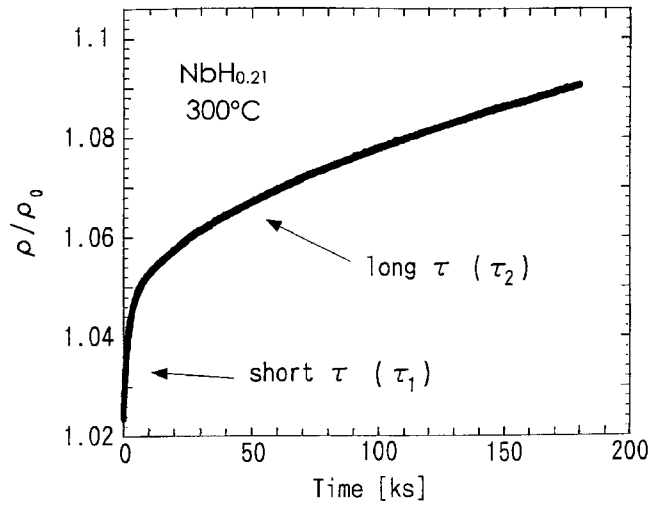


**Figure 1.** Temporal variation of the electrical resistivity of a single-crystalline sample of NbH<sub>0.21</sub> at 300 °C normalized to  $\rho_0$  at  $t = 0$ . The resistivity increases in two stages, a fast stage with a small time constant ( $\tau_1$ ) and a slow stage with a large time constant ( $\tau_2$ ).

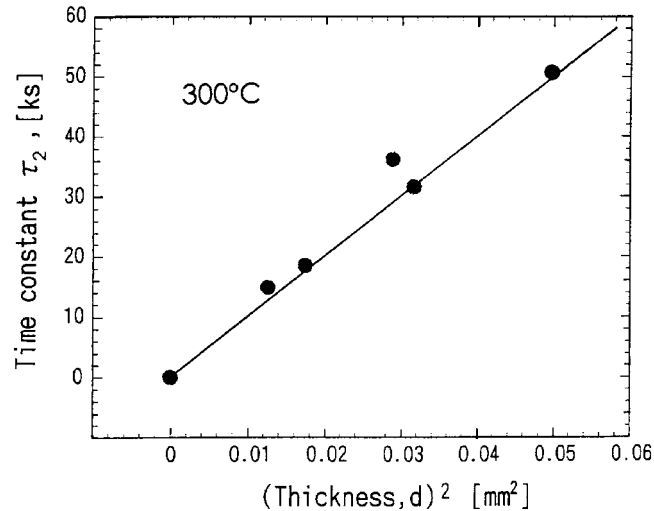


**Figure 2.** The time constant of the slow stage  $\tau_2$  plotted against the sample thickness squared,  $d^2$ . Measurements were made at 300 °C on single-crystalline samples of H/Nb = 0.11–0.61.

$\Delta\rho_2(t)$  is the slow component due to vacancy migration from the surface of a plate [26]

$$\Delta\rho_2(t) \approx \Delta\rho_2 \left[ 1 - 0.811(e^{-t/\tau_2} + \frac{1}{9}e^{-9t/\tau_2}) \right] \quad (2)$$

and  $\Delta\rho_{ox}(t)$  is a small correction expressed as a linear increase with time. The origin of  $\Delta\rho_{ox}(t)$  was not identified, but its presence even in pure Nb suggests that it is due to the effect of incipient oxidation.

As shown in figure 2, the time constant  $\tau_2$  is proportional to the sample thickness squared:

$$\tau_2 \approx 1.0 \times 10^3 (d \text{ (mm)})^2 \text{ (ks)}.$$

This is an unambiguous proof that the slow process is rate-controlled by diffusion from the surface into the interior. On the other hand, the observed small time constant was in the range

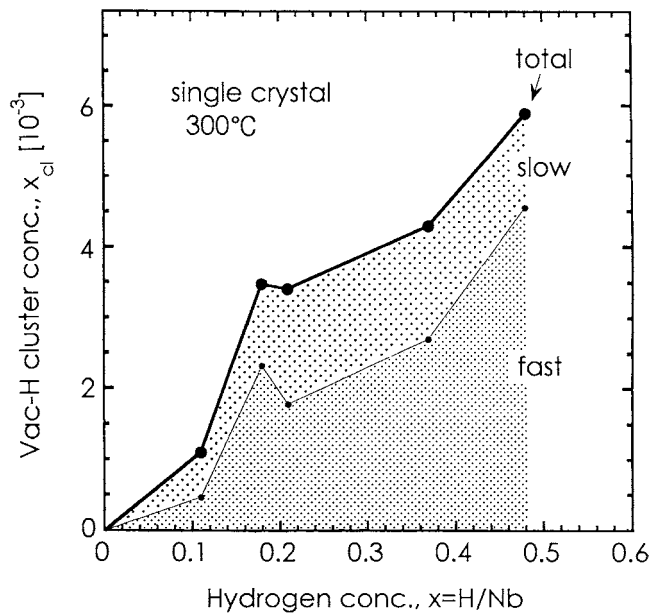


**Figure 3.** Vacancy–H cluster concentration  $x_{cl}$  at 300 °C plotted against H concentration  $x = H/Nb$ . The cluster concentrations have been estimated from observed resistivity increments. The total cluster concentration and its breakdown into fast and slow components are shown.

of  $\tau_1 = 1 \pm 0.4$  ks, without any correlation with the sample thickness. This is consistent with vacancy formation from sources distributed uniformly in the sample.

The resistivity increments measured at 300 °C can be converted into the vac–H cluster concentration  $x_{cl}$  if the resistivity per unit concentration of vac–H clusters is known. In the absence of this knowledge, we approximate it by 1/2 of the Frenkel-pair resistivity in Nb:  $\rho_{vac} = 7 \pm 1.5 \mu\Omega \text{ cm/at.}\%$  [24]. Possible conversion errors may be expected to be less than a factor of 2. The vac–H cluster concentrations estimated in this way for different H concentrations are shown in figure 3. Within the scatter of data points, the dependence of the total cluster concentration  $x_{cl}$  on H concentration  $x$  can be deemed linear in this concentration range;  $x_{cl} \approx 1.3 \times 10^{-2}x$ .

### 3.2. Temperature dependence of the vacancy formation process

To investigate the temperature dependence of the vacancy formation process, similar measurements were made on samples of NbH<sub>0.26</sub> at temperatures between 200 and 300 °C. The Arrhenius plots of the time constants  $\tau_1$  and  $\tau_2$  are shown in figure 4. The temperature dependence for the fast process can be well represented by

$$\tau_1 = 3.6 \times 10^{-1} \exp\left(\frac{0.33 \text{ eV}}{kT}\right) \text{ (s)}, \quad (3)$$

and for the slow process by

$$\tau_2 = 9.4 \times 10^{-3} \exp\left(\frac{0.75 \text{ eV}}{kT}\right) \text{ (s)}. \quad (4)$$

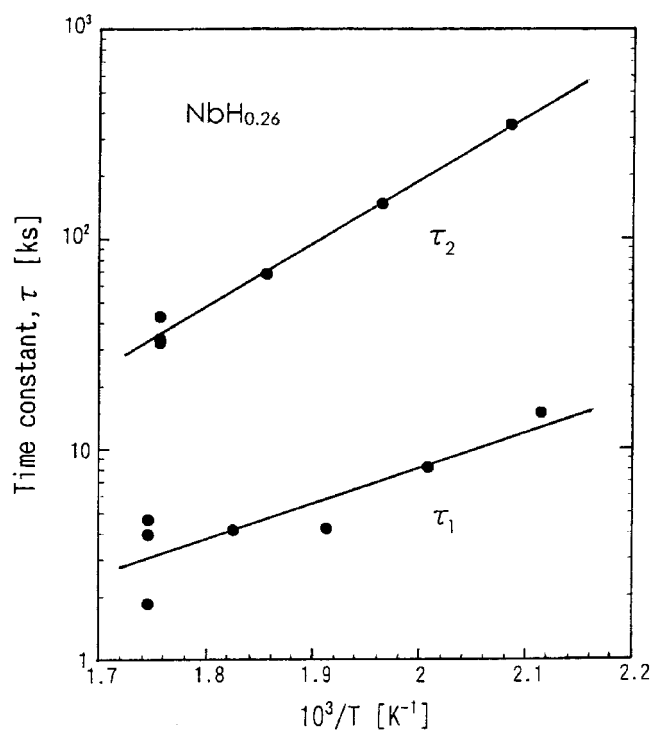


**Figure 4.** The Arrhenius plot of the time constant of the fast process  $\tau_1$  and of the slow process  $\tau_2$  in a single-crystalline sample of  $\text{NbH}_{0.26}$ .

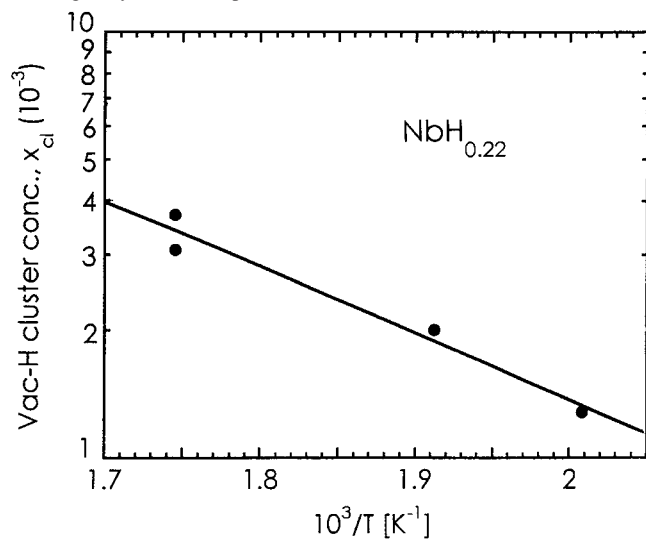


**Figure 5.** The Arrhenius plot of the vac-H cluster concentration  $x_{cl}$  in a single-crystalline sample of  $\text{NbH}_{0.22}$ .

The Arrhenius plot of the (total) cluster concentration is shown in figure 5. The best-fit line gives

$$x_{cl} = 1.7 \exp\left(\frac{-0.30 \text{ eV}}{kT}\right), \quad (5)$$

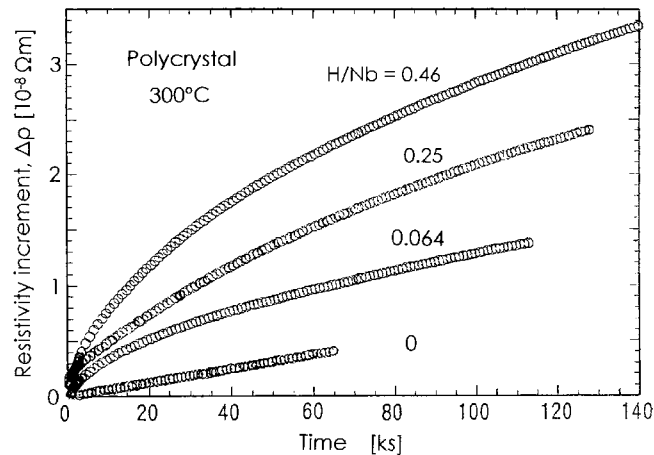


**Figure 6.** Temporal variation of the resistivity increment of polycrystalline samples of NbH<sub>0.46</sub>, NbH<sub>0.25</sub>, NbH<sub>0.064</sub> and Nb, measured at 300 °C.

which, allowing for fairly large uncertainties, is better written as

$$x_{cl} \approx 2 \times 10^{\pm 1} \exp\left(\frac{-(0.3 \pm 0.1) \text{ eV}}{kT}\right). \quad (6)$$

In spite of large uncertainties due to the limited number of data points and available range of temperature, a drastic reduction of the vacancy formation energy from the value in Nb ( $e_f^v \approx 3.07 \text{ eV}$  [24]) is obvious.

The temporal variation of the resistivity measured at 300 °C for polycrystalline samples of different H concentrations is illustrated in figure 6. The linear increase in pure Nb, which is more conspicuous in polycrystalline than in single-crystalline samples, is believed to be due to gradual dissolution of oxygen atoms by short-circuit diffusion through dislocations and/or grain boundaries. Unlike the case for single-crystalline samples (figure 1), only the slow process is observed here.

The Arrhenius plot of the time constant for a polycrystalline wire of NbH<sub>0.5</sub> is shown in figure 7. The best-fit relation is expressed as

$$\tau_2 = 3.5 \times 10^{-2} \exp\left(\frac{0.82 \text{ eV}}{kT}\right) \text{ (s)}, \quad (7)$$

which gives the activation energy in reasonable agreement with that of a single crystal (equation (4)).

The concentration of vac–H clusters estimated from the observed resistivity increment is shown in figure 8 as a function of H concentration. In comparison to single-crystal data (figure 3), the apparent cluster concentrations in polycrystalline samples are smaller, especially at high H concentrations. This points to the possibility that the fast process, though actually existing, escaped observation because it was too fast.

### 3.3. Pressure dependence of the vacancy formation process

The pressure dependence of the vacancy formation process in single-crystalline samples of NbH<sub>0.22</sub> was measured at 300 °C under three different pressures between 2 and 4 GPa. The temporal variation of the resistivity increment measured at 3 GPa is shown in figure 9. As seen in the figure, the scatter of data points in high-pressure experiments is larger, but still



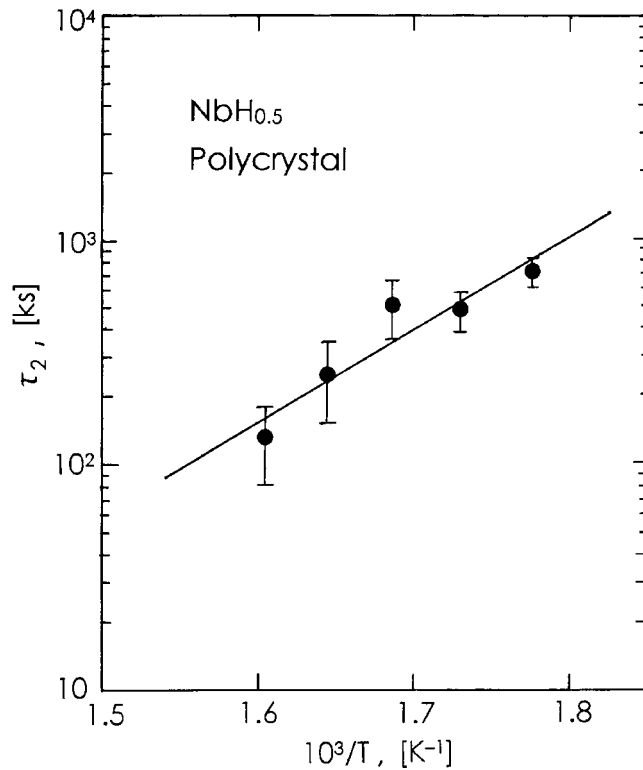


**Figure 7.** The Arrhenius plot of the time constant of the slow process  $\tau_2$  in a polycrystalline sample of  $\text{NbH}_{0.5}$ .

admissible. The plot of  $\lg \tau$  versus pressure is shown in figure 10. The three high-pressure data and the value of  $\tau_1$  at  $p = 0$  form a fairly good straight line, indicating that the process observed at high pressures is in fact the fast process due to the introduction of vac-H clusters from internal sources. The best-fit line can be represented by

$$\tau_1 = 1.4 \times 10^3 \exp(0.66p \text{ (GPa)}) \text{ (s)}. \quad (8)$$

As this implies that  $p v_m^{\text{cl}}/kT = 0.66p \text{ (GPa)}$  at  $300^\circ\text{C}$ , the activation volume for the migration of a vac-H cluster can be obtained as  $v_m^{\text{cl}} = 5.2 \text{ \AA}^3$ .

Figure 11 shows the data obtained for polycrystalline samples of  $\text{NbH}_{0.6}$  under 5 GPa, at three representative temperatures. (These are the data obtained before the system of automatic resistometry was introduced, and therefore involve larger scatters.) Here again, only the fast process was observed. The Arrhenius plot of the time constant, shown in figure 12, gives

$$\tau_1 \approx 1 \times 10^{-3} \exp\left(\frac{0.46 \pm 0.05 \text{ eV}}{kT}\right) \text{ (s)}. \quad (9)$$

This indicates that, due to the increase of the activation enthalpy at high pressures, the fast process has slowed down to become barely observable, while the slow process has become too slow to be observed. Indeed, using the activation volume of  $v_m^{\text{cl}} = 5.2 \text{ \AA}^3$ , the time constant at  $300^\circ\text{C}$  is estimated to be 26 times longer at 5 GPa than at 0 GPa. Thus in polycrystals, the fast process at 0 GPa becomes too fast, and the slow process at 5 GPa too slow to be observed, in agreement with the observation. The increase of the activation enthalpy by  $0.13 \pm 0.05 \text{ eV}$  at

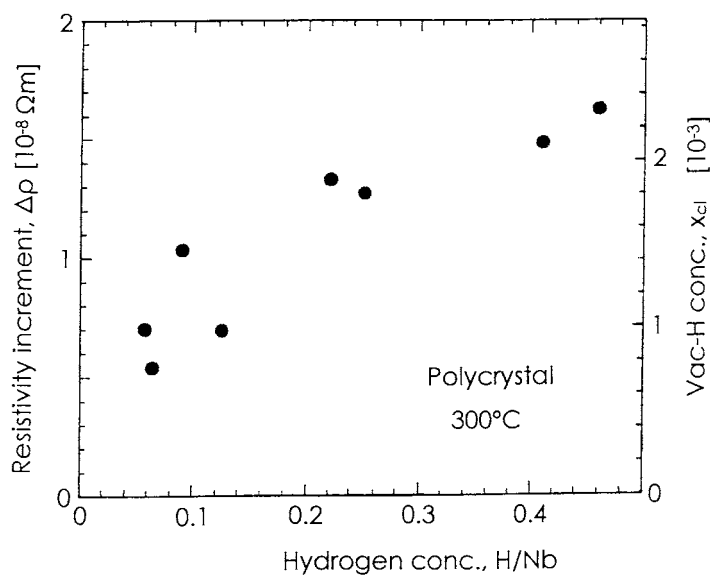


**Figure 8.** Resistivity increments in the slow process and vac–H concentrations estimated therefrom for polycrystalline samples of various H concentrations, measured at 300 °C.

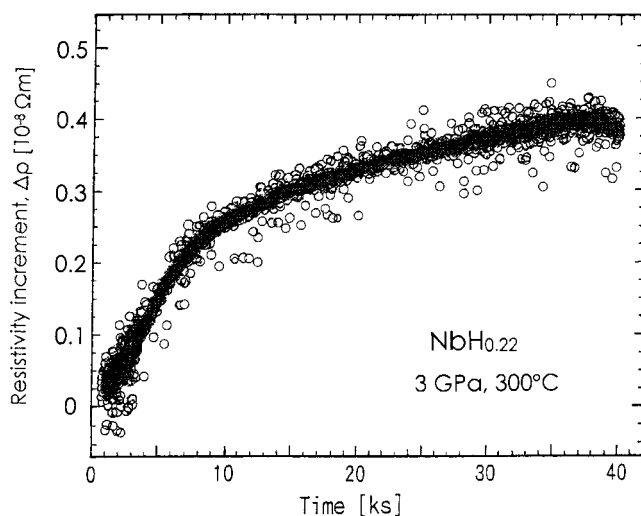


**Figure 9.** The temporal variation of the resistivity increment of a single-crystalline sample of NbH<sub>0.22</sub> at 300 °C, measured under 3 GPa.

5 GPa (cf equations (3) and (9)) is consistent with  $pv_m^{\text{cl}} = 0.16 \text{ eV}$  estimated from  $v_m^{\text{cl}} = 5.2 \text{ \AA}^3$ . The concentration of vac–H clusters in polycrystalline samples is shown in figure 13 as a function of temperature. Again the concentrations are smaller than the equilibrium value in single crystals because in this case an additional supply from the external surface was yet to be attained.

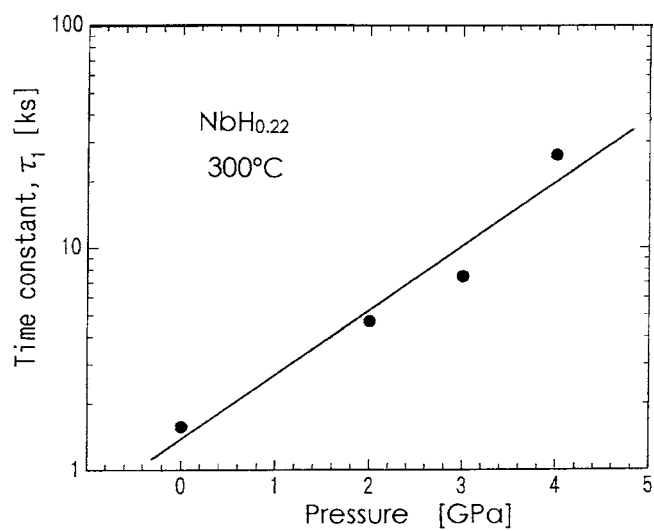


**Figure 10.** The pressure dependence of the time constant of the fast process  $\tau_1$  in a single-crystalline sample of  $\text{NbH}_{0.22}$  at 300 °C.

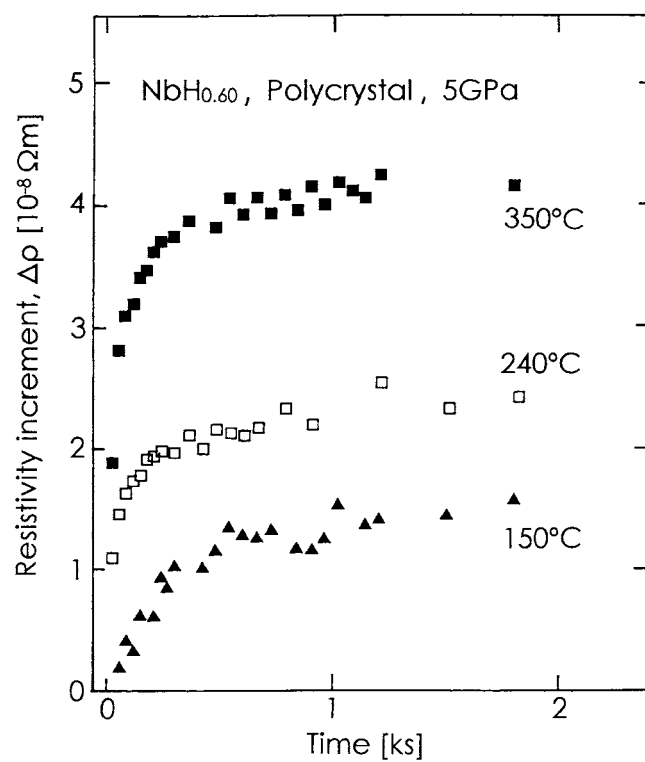


**Figure 11.** The temporal variation of the resistivity increment of polycrystalline samples of  $\text{NbH}_{0.60}$ . Measurements were made under 5 GPa, at three different temperatures, 150, 240 and 350 °C.

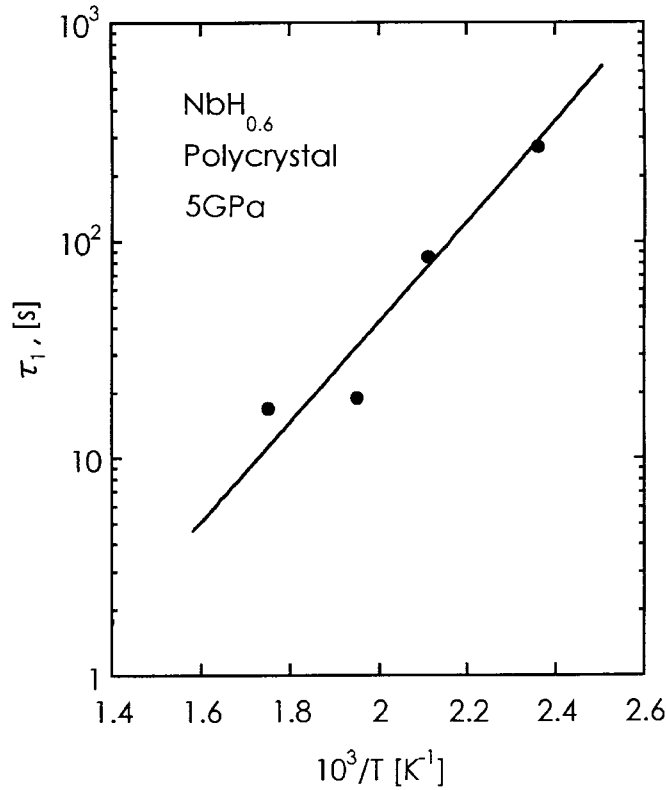


**Figure 12.** The Arrhenius plot of the time constant of the fast process  $\tau_1$  in a polycrystalline sample of NbH<sub>0.60</sub> measured under 5 GPa.

#### 4. Discussion

The diffusion coefficient of vac–H clusters can be obtained from  $\tau_2$  using the relation appropriate for a planar sample [26]:

$$D^{\text{cl}} = \frac{d^2}{\pi^2 \tau_2} = 3.1 \times 10^{-7} e^{-0.75 \text{ eV}/kT} \text{ (m}^2 \text{ s}^{-1}\text{)}. \quad (10)$$

Writing  $D^{\text{cl}} = D_0^{\text{cl}} \exp(-e_m^{\text{cl}}/kT)$ , and comparing with the expression for the diffusivity of a vacancy in Nb,  $D^{\text{v}} = D_0^{\text{v}} \exp(-e_m^{\text{v}}/kT)$ , where  $D_0^{\text{v}} \approx 10^{-5} \text{ m}^2 \text{ s}^{-1}$  and  $e_m^{\text{v}} = 0.55 \text{ eV}$  [24], we note that the pre-exponential factor becomes smaller and the migration energy becomes larger for a vac–H cluster. Writing  $D_0^{\text{cl}} = D_0^{\text{v}} \exp(\Delta s_m/k)$  and  $e_m^{\text{cl}} = e_m^{\text{v}} + \Delta e_m$ , we obtain  $\Delta s_m/k \approx -3.5$  and  $\Delta e_m = 0.20 \text{ eV}$ . The increase of the migration energy is comparable to the migration energy of an H atom  $e_m^{\text{H}} = 0.13 \text{ eV}$  in NbH<sub>0.2</sub> [27]. Very similar changes of  $s_m$  and  $e_m$  were observed for the migration of vac–H clusters in Pd–H alloys [9].

The activation volume  $v_m^{\text{cl}} = 5.2 \text{ \AA}^3$  obtained from the pressure dependence of the fast process assumes a ratio to the atomic volume  $v_m^{\text{cl}}/\Omega_0 = 0.26$ , which lies in the range generally accepted for the migration of a vacancy  $v_m^{\text{v}}/\Omega_0 = 0.2\text{--}0.3$  [24].

The fact that the time constant of the fast process is independent of the sample thickness suggests that it is rate-controlled by diffusion over distances which are nearly the same in all the samples. Using  $\tau_1 \sim 1 \pm 0.4 \text{ ks}$ , and  $D^{\text{cl}} \approx 8 \times 10^{-14} \text{ m}^2 \text{ s}^{-1}$  at 300 °C (equation (10)), the diffusion distance can be estimated as  $l \sim \sqrt{D^{\text{cl}} \tau_1} = 9 \times 10^{-6} \text{ m}$ . This value is reasonable

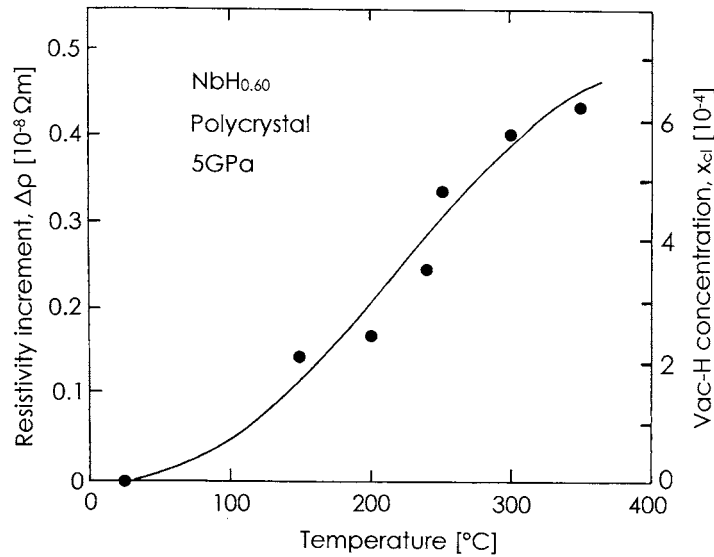


**Figure 13.** Resistivity increments in the fast process and vac-H concentrations estimated therefrom in polycrystalline samples of NbH<sub>0.60</sub>. Measurements were made under 5 GPa at several different temperatures.

for an average distance between dislocations;  $N_d = 1/l^2 \sim 10^{10} \text{ m}^{-2}$  is of the order of magnitude expected for well-annealed crystals. In polycrystals, from  $\tau_1 \sim 20 \text{ s}$  at 300°C and 5 GPa (figure 12), the value at 0 GPa is estimated to be  $\tau_1 \sim 1 \text{ s}$ , which is  $10^3$  times shorter than in a single crystal. The dislocation density required to explain this difference amounts to  $N_d \sim 10^{13} \text{ m}^{-2}$ , which is again not unreasonable for a cold-drawn wire. In this model calculation, we are assuming in effect that vacancies are transported from the surface to the interior by fast diffusion along dislocations, and subsequently from dislocations to the surrounding lattice by bulk diffusion; this latter constitutes the rate-limiting step of the fast process. Certainly, grain boundaries should have provided easier paths for vacancy diffusion, as demonstrated clearly in Ni-H alloys by microscopic observations of coagulated vacancies (nanopores) along the grain boundaries [28], but the rate-determining step in the present case should still be the diffusion into each grain (several tens of microns in size) with the aid of a dislocation network (of average spacing  $\sim 0.3 \mu\text{m}$ ). As vacancies supplied by the fast process amount to  $x_{cl} \leq 10^{-2}$ , it is hardly conceivable that any built-in defects could possess such large capacities. Dislocations can produce vacancies by climb motion, but their capacity should be very much smaller, especially at the temperatures of the present experiment. No other defects could possibly act as such regenerative, almost inexhaustible vacancy sources.

From the observed reduction of the vacancy formation energy in the presence of interstitial H atoms, the average energy of binding of an H atom to a vacancy can be estimated. If we assume that six H atoms are trapped by a vacancy, probably in the vicinity of the nearest octahedral sites, the average binding energy can be calculated as  $e_b \approx (3.07 - 0.3) - 6 = 0.46 \text{ eV}$ .<sup>2</sup> This value compares reasonably well with the experimental value  $e_b = 0.55 \text{ eV}$ ,

<sup>2</sup> The formation energy of a vacancy  $e_f^v = 3.07 \text{ eV}$  was obtained from the difference of the activation energy of self-diffusion  $e_{SD} = 3.62 \text{ eV}$  and the migration energy of a vacancy  $e_m^v = 0.55 \text{ eV}$ . This value is preferred to  $2.6 \pm 0.3 \text{ eV}$  obtained from positron annihilation experiments [24].

obtained from positron lifetime spectroscopy for a single H atom trapped by a vacancy [29]<sup>3</sup>. The binding energy of  $\sim 0.59$  eV was predicted by a calculation based on the effective-medium theory for up to six H atoms around a vacancy in Nb [30]. At the temperatures of the present experiment, it is reasonable to assume that H atoms are trapped up to a maximum possible number, and the degree of detrapping is negligibly small.

It must be admitted, however, that from the present experiment alone, six H atoms being trapped by a vacancy does not follow uniquely, although it appears coherent with the reported values of the binding energy. The trapping of 12 H atoms with the average binding energy of 0.23 eV, for example, explains the present observation equally well. The possibility of more than six H atoms being trapped by a vacancy, especially in metals with a large atomic volume such as Nb, was in fact briefly mentioned in [30], but has not been examined further.

The dependence of  $x_{cl}$  on the H concentration  $x$  deserves special consideration. In our previous paper, we developed a theory describing the chemical equilibrium between the vacancy and interstitial H atoms, and reached an expression in which the equilibrium concentration of  $\text{vacH}_6$  clusters is proportional to  $x^6$ . This is in apparent contradiction to the  $x$ -dependence observed in the present experiment. The source of this discrepancy lies in the approximations that the Boltzmann statistics was adopted and the configurational entropy was calculated for low-concentration limits of vacancies and H atoms. Neither of these approximations is valid in the present experimental conditions. To explain the nearly linear  $x$ -dependence observed, further considerations appropriate for the actual experimental conditions are needed.

From the pressure dependence of the equilibrium cluster concentration, a crude estimate of the formation volume of a  $\text{vac-H}$  cluster  $v_f^{cl}$  can be obtained. For a H concentration of  $x = 0.22$  at 300 °C, the cluster concentration at 3 GPa shown in figure 9 is 0.06 at.%, which is nearly 1/4 of the value at 0 GPa shown in figure 3 (or slightly larger than this if a slow component is included). The formation volume is thus estimated to be  $v_f^{cl} = 3.7 \text{ \AA}^3$ , i.e.  $v_f^{cl}/\Omega_0 = 0.18$  (or even smaller). Considering that the formation volume of a vacancy in Nb satisfies  $v_f^v/\Omega_0 = 0.7$ , as in many other metals [31], this value of  $v_f^{cl}$  is exceptionally small. This result may be rationalized by assuming that the volume expansion caused by interstitial H atoms, which is  $\Omega_H = 2.8 \text{ \AA}^3/\text{H atom}$  in Nb [32, 33], becomes smaller for trapping by vacancies. Writing  $v_f^{cl} = v_f^v + 6\Delta\Omega_H$  and substituting in  $v_f^{cl} = 3.7 \text{ \AA}^3$  and  $v_f^v \approx 14 \text{ \AA}^3$ , we obtain  $\Delta\Omega_H = -1.7 \text{ \AA}^3/\text{H atom}$ . The H-induced volume is reduced to nearly 40% in the trapped state. If we assumed instead  $v_f^{cl} \approx v_f^v = 14 \text{ \AA}^3$  (i.e.  $v_f^{cl}/\Omega_0 = 0.7$ ), the equilibrium cluster concentration under 3 GPa would become  $\sim 1/200$  of the zero-pressure value, hardly observable in the present experiment. This small formation volume is believed to be a common feature of  $\text{vac-H}$  clusters in M–H alloys, and underlies the formation of superabundant vacancies under high pressures, actually observed in our previous experiments.

In closing the discussion, a brief description will be given of the result of temporary interruption of the cluster formation process. Figure 14 shows the resistivity change of a polycrystalline wire of  $\text{NbH}_{0.46}$  during heating at 320 °C, with a temporary interruption for 2 ks. The result shows that, after the temporary cooling to room temperature, the resistivity recovered to its value before the interruption. The effect of 320 °C holding prior to the interruption was perfectly memorized. On a closer look, we note that it takes a few kiloseconds for the resistivity to recover the value at 320 °C. The process involved here is believed to be as follows: as  $\text{vac-H}$  clusters have an equilibrium concentration 300 times higher at 320 °C

<sup>3</sup> From the temperature dependence of the lifetime of positrons trapped by vacancies in electron-irradiated Nb, it was found that the starting temperature of vacancy migration was 190 K, and this was shifted to 380 K in the presence of interstitial H atoms. As the ratio of these two temperatures gives the ratio of activation energies  $e_m^v$  and  $e_m^v + e_b$ ,  $e_m^v = 0.55$  eV gives  $e_b = 0.55$  eV. The assignment made by the authors of the latter energy to  $e_m^H + e_b$  is not correct.

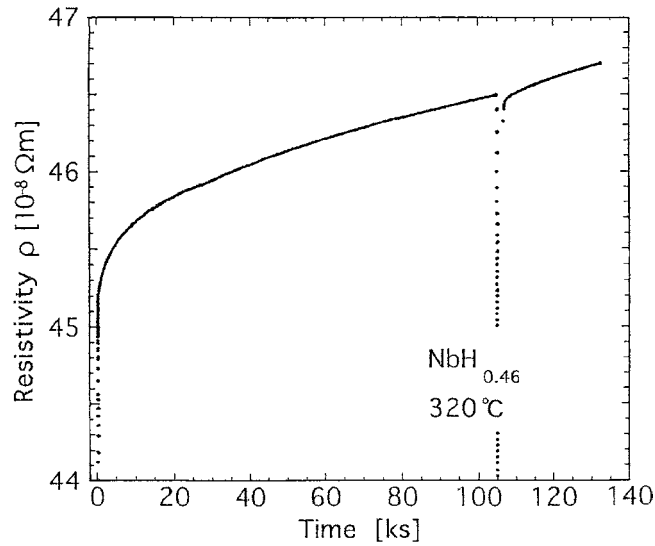


**Figure 14.** The temporal variation of the electrical resistivity in polycrystalline NbH<sub>0.46</sub> at 320 °C. After a temporary cooling to room temperature for 2 ks, the resistivity returned in a few kiloseconds to its value before the interruption.

than at room temperature, upon quenching they precipitate to form microvoids, which upon reheating re-dissolve in the matrix. (Due to difficulties in controlling the ‘room temperature’ in the quenched state, meaningful comparison of the resistivities in the initial and quenched states was not possible.) These results show that the kinetics of SAV formation is a highly structure-sensitive property. In order to obtain reproducible results on the SAV formation, we have to start with well-defined initial conditions. This precaution was taken in the present experiment by using specimens cut out from the same piece, and carefully prepared at room temperature to avoid introducing plastic deformations, i.e. additional dislocations.

One of the most conspicuous effects of SAV formation is the enhancement of metal-atom diffusion. Although the diffusivity of vacancies is reduced by trapping H atoms, the drastic enhancement of their equilibrium concentration more than offsets the reduction, and results in the enhancement of M-atom diffusion. The H-induced enhancement of interdiffusion was reported in our previous papers for Pd–Rh alloys [5] and Cu/Ni diffusion couples [25] as evidence of this effect, but with some complications due to thermodynamic properties of the ternary system, namely the effect of H on the thermodynamical factor. The enhancement of interdiffusion was also observed in Fe/Fe–Au diffusion couples [34]. Recently, the H-induced enhancement of self-diffusion was observed in Nb, a more clear-cut demonstration of the effect of SAV formation, the result of which will be reported in our forthcoming paper.

## 5. Summary and conclusions

The formation of superabundant vacancies (SAVs), of concentrations amounting to  $\leq 1$  at.%, has been observed by measuring the electrical resistivity of Nb–H alloys at  $\leq 350$  °C. In the SAV formation process, the fast diffusion along dislocations usually dominates over bulk diffusion from the external surface, especially in polycrystalline samples. From the temperature and pressure dependence of the kinetics and equilibrium concentration of SAVs (vac–H clusters), the activation energy and the activation volume of migration and formation of

vac–H clusters have been obtained, and explained tentatively in terms of trapping of six H atoms per vacancy.

### Acknowledgments

We wish to thank H Hiraoka for his cooperation in the initial stage of this experiment. This work was supported by a Grant-in-Aid for Scientific Research from the Ministry of Education, Science and Culture.

### References

- [1] Fukai Y and Ōkuma N 1993 *Japan. J. Appl. Phys.* **32** L1256
- [2] Fukai Y and Ōkuma N 1994 *Phys. Rev. Lett.* **73** 1640
- [3] Ōsono H, Kino T, Kurokawa Y and Fukai Y 1995 *J. Alloys Compounds* **231** 41
- [4] Nakamura K and Fukai Y 1995 *J. Alloys Compounds* **231** 46
- [5] Watanabe K, Ōkuma N, Fukai Y, Sakamoto Y and Hayashi Y 1996 *Scr. Mater.* **34** 551
- [6] Iwamoto M and Fukai Y 1999 *Trans. Japan Inst. Met.* **40** 606
- [7] Birnbaum H K, Buckley C, Zaides F, Sirois E, Rosenak P, Spooner S and Lin J S 1997 *J. Alloys Compounds* **253/254** 260
- [8] dos Santos D S, Miraglia S and Fruchart D 1999 *J. Alloys Compounds* **291** L1
- [9] Fukai Y, Ishii Y, Goto T and Watanabe K 2000 *J. Alloys Compounds* **313** 121
- [10] Miraglia S, Fruchart D, Hlil E K, Tavares S S M and dos Santos D 2001 *J. Alloys Compounds* **317** 77
- [11] Fukai Y, Haraguchi T, Hayashi E, Ishii Y, Kurokawa Y and Yanagawa J 2001 *Defect Diffusion Forum* **194** 1063
- [12] Fukai Y, Shizuku Y and Kurokawa Y 2001 *J. Alloys Compounds* **329** 195
- [13] Fukai Y and Mizutani M 2002 *Mater. Trans.* **43** 1079
- [14] Fukai Y, Mori K and Shinomiya H 2003 *J. Alloys Compounds* **348** 105
- [15] Fukai Y and Mizutani M 2003 *Mater. Trans.* **44** 1359
- [16] Fukai Y, Mizutani M, Yokota S, Kanazawa M, Miura Y and Watanabe T 2003 *J. Alloys Compounds* **356/357** 270
- [17] Fukai Y 1995 *J. Alloys Compounds* **231** 35
- [18] Fukai Y, Kurokawa Y and Hiraoka H 1997 *J. Japan Inst. Metals* **61** 663
- [19] Fukai Y 2003 *J. Alloys Compounds* **356/357** 263
- [20] Fukai Y 2003 *Phys. Scr. T* **103** 11
- [21] Myers S M, Richards P M, Wampler W R and Besenbacher F 1989 *J. Nucl. Mater.* **165** 9
- [22] Myers S M, Baskes M I, Birnbaum H K, Corbett J W, DeLeo G G, Estreicher S K, Haller E E, Jena P, Johnson N M, Kirchheim R, Pearton S J and Stavola M J 1992 *Rev. Mod. Phys.* **64** 559
- [23] Myers S M, Nordlander P, Besenbacher F and Nørskov J K 1986 *Phys. Rev. B* **33** 851
- [24] Ehrhart P, Jung P, Schultz H and Ullmaier H 1991 *Atomic Defects in Metals (Landolt–Börnstein New Series vol 25)* ed P Ullmaier (Berlin: Springer)
- [25] Hayashi E, Kurokawa Y and Fukai Y 1998 *Phys. Rev. Lett.* **80** 5588
- [26] Crank J 1975 *The Mathematics of Diffusion* (Oxford: Clarendon)
- [27] Sevilla E H and Cotts R M 1988 *Phys. Rev. B* **37** 6813
- [28] dos Santos D S, Tavares S S M, Miraglia S, Fruchart D and dos Santos D R 2003 *J. Alloys Compounds* **356/357** 258
- [29] Hautojärvi P, Huomo H, Puska M and Vehanen A 1985 *Phys. Rev. B* **32** 4326
- [30] Nordlander P, Nørskov J K, Besenbacher F and Myers S M 1989 *Phys. Rev. B* **40** 1990
- [31] Korzhavyi P A, Abrikosov I A, Johansson B, Ruban A V and Skriver H L 1999 *Phys. Rev. B* **59** 11693
- [32] Peisl H 1978 *Hydrogen in Metals I* ed G Alefeld and J Völkl (Berlin: Springer)
- [33] Fukai Y 1993 *The Metal Hydrogen System* (Berlin: Springer)
- [34] Yamazaki Y, Iijima Y and Okada M 2004 *Acta Materialia* at press